substance: Ti_nO_{2n-1} ($n \geq 3$)
property: transport properties

conductivity: for Ti_3O_5: Fig. 1; Ti_4O_7: Fig. 2, 3; Ti_5O_9: Fig. 4, 5; Ti_6O_{11}: Fig. 6, 7; Ti_7O_{13}: Fig. 8; Ti_8O_{15}: Fig. 9; Ti_9O_{17}: Fig. 10.

The following table [75H] presents a comparison of calculated and measured values of the conductivity and the carrier mobility, the hopping frequencies f_h and mobilities μ_h and concentrations as well as effective masses of localized (n_{loc}) and delocalized (n_{del}) electrons.

transport parameters

$\sigma_{exp}[\Omega^{-1}\ cm^{-1}]$	$5.5\cdot10^{-3}$	Ti_3O_5	low-temperature phase (see also	69B
	$3.10\cdot10^{-3}$	Ti_4O_7	Figs. 1, 2). T = 120 K. σ measured	
	6.3	Ti_5O_9	along *b*-axis of single crystal	
	$7.0\cdot10^{-2}$	Ti_6O_{11}	sample; [77M] gives σ two orders of magnitude lower for Ti_5O_9	
	$2.5\cdot10^{-1}$	Ti_8O_{15}	no phase transition	
$\sigma_{exp}[\Omega^{-1}\ cm^{-1}]$	$3.5\cdot10^{1}$	Ti_3O_5	high-temperature phase;	69B
	$1.5\cdot10^{3}$	Ti_4O_7	T = 450 K for Ti_3O_5 and 300 K	
	$5.5\cdot10^{2}$	Ti_5O_9	for the others; [77M] again	
	$1.1\cdot10^{2}$	Ti_6O_{11}	reports significantly lower conductivity for Ti_5O_9 at 300 K ($\approx 0.6\ \Omega^{-1}\ cm^{-1}$)	
$\mu_{calc}[cm^2/V\ s]$	0.21	Ti_3O_5	T = 450 K	75H
	0.6	Ti_4O_7	T = 300 K	
	4.1		T = 160 K	
	0.76	Ti_5O_9	T = 300 K	
	0.9	Ti_6O_{11}	T = 300 K	
$\mu_{exp}[cm^2/Vs]$	1.0	Ti_4O_7	T = 300 K	75H
	4.0		T = 160K	
f_h[Hz]	$4.9\cdot10^{11}$	Ti_3O_5	T = 120K	75H
	$1.6\cdot10^{12}$	Ti_4O_7		
	$9.3\cdot10^{12}$	Ti_5O_9		
	$1.4\cdot10^{13}$	Ti_6O_{11}		
	$1.5\cdot10^{12}$	Ti_8O_{15}		
$\mu_h[cm^2/V\ s]$	$7.0\cdot10^{-5}$	Ti_3O_5	T = 120 K	75H
	$4.0\cdot10^{-6}$	Ti_4O_7		
	$4.2\cdot10^{-4}$	Ti_5O_9		
	$2.7\cdot10^{-7}$	Ti_6O_{11}		
	$2.1\cdot10^{-4}$	Ti_8O_{15}		

n_{loc}[cm^{-3}]	0.00	Ti_3O_5	high-temperature region,	75H
	$1.71 \cdot 10^{21}$	Ti_4O_7	calculated from magnetic	
	$1.10 \cdot 10^{21}$	Ti_5O_9	susceptibility (T = 450 K for Ti_3O_5	
	$3.7 \cdot 10^{21}$	Ti_6O_{11}	and 300 K for the others)	
	$3.85 \cdot 10^{21}$	Ti_8O_{15}		
n_{del}[cm^{-3}]	$2.29 \cdot 10^{22}$	Ti_3O_5	high-temperature region,	75H
	$1.54 \cdot 10^{22}$	Ti_4O_7	calculated from magnetic	
	$1.24 \cdot 10^{22}$	Ti_5O_9	susceptibility (T as above)	
	$7.4 \cdot 10^{21}$	Ti_6O_{11}		
	$4.6 \cdot 10^{21}$	Ti_8O_{15}		
n_{del}[cm^{-3}]	$9.1 \cdot 10^{20}$	Ti_3O_5	low-temperature region, from	75H
	$2.4 \cdot 10^{21}$	Ti_4O_7	EPR data; T = 120 K< T_{tr}, except	
	$1.7 \cdot 10^{21}$	Ti_5O_9	for Ti_8O_{15}, where no T_{tr} were	
	$3.8 \cdot 10^{21}$	Ti_6O_{11}	observed	
	$5.3 \cdot 10^{21}$	Ti_8O_{15}		
m_n/m_0	22.4 (6.7)	Ti_3O_5	high-temperature region,	75H
	15.4 (5.6)	Ti_4O_7	in brackets: low temperature-	
	19.5 (6.4)	Ti_5O_9	region defined above	
	15.4 (5.4)	Ti_6O_{11}		
	13.2 (12.5)	Ti_8O_{15}		

further transport data and remarks

[76L] finds that σ increases in Ti_4O_7 between 160 and 300 K in a similar way to that reported by [69B] for Ti_5O_9. [83I] reports both types of behaviour depending on the crystal orientation. For one free electron per Ti^{3+} calculated mobilities are 0.55 cm^2/V s [69B], 0.05 cm^2/V s [76L] at 300 K. Below T_{tr} no activation energies can be obtained for Ti_3O_5, Ti_4O_7, Ti_5O_9, Ti_6O_{11}.

However, Ti_8O_{15} shows no transition and an activation energy of 0.087 eV. In Ti_3O_5, the transition involves a structural rearrangement in which Ti^{3+} – Ti^{3+} bonds are broken at high temperatures and the electrons become quasi-itinerant. The two transitions seen in Ti_4O_7 and Ti_5O_9 have been ascribed to solid-liquid-gas. The central unit remains a Ti^{3+} – Ti^{3+} bond in the intermediate phase, but this "bipolaron" becomes mobile. The Seebeck coefficient suggests n-type conduction [79S], and in the low-temperature region variable-range hopping occurs [79S]. [83I] reports fine structure in the hysteresis range of Ti_4O_7 (Fig. 3) and three transitions, at 127(2), 132(1) and 139(1) K in the conductivity of Ti_5O_9 (Fig. 5). Unlike [69B], who reports a transition at 130 K in Ti_6O_{11}, [83I] reports two transitions, at 119(1) and 147(1) K (Fig. 7). Interestingly, Ti_7O_{13} appears to show no metallic region (Fig. 8), but a transition at 115 K↓, 123 K↑ between two semiconducting regions. Below T_{tr} for n = 5, 6 or 7, ln σ varies linearly with T, a result ascribed to temperature-dependent incoherent tunneling [83I].

References:

69B Bartholomew, R. F., Frankl, D. R.: Phys. Rev. 187 (1969) 828.
75H Houlihan, J. F., Danley, W. J., Mulay, L. N.: J. Solid State Chem. 12 (1975) 265.
76L Lakkis, S., Schlenker, C., Chakraverty, B. K., Buder, R., Marezio, M.: Phys. Rev. B14 (1976) 1429.
77M Marezio, M., Tranquin, D., Lakkis, S., Schlenker, C.: Phys. Rev. B16 (1977) 2811.
79S Schlenker, C., Ahmed, S., Buder, R., Gourmala, M.: J. Phys. C12 (1979) 3503.
83I Inglis, A. D., LePage, Y., Strobel, P., Hurd, C. M.: J. Phys. C16 (1983) 317.

Fig. 1.

Ti_3O_5. Conductivity along *b*-axis vs. (reciprocal) temperature of single crystal material [69B].

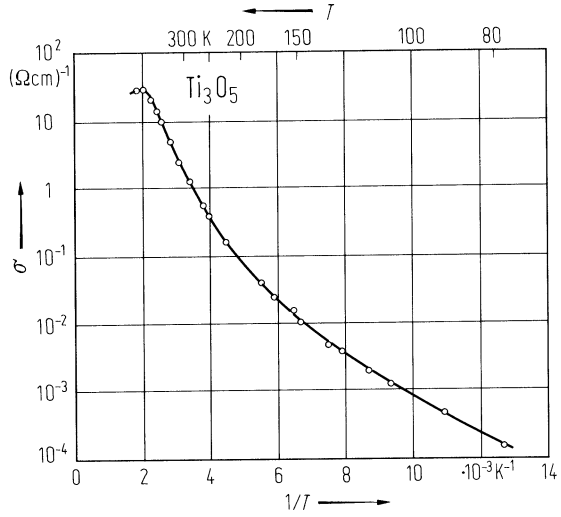

Fig. 2.

Ti_4O_7. Conductivity along [031] pseudorutile direction vs. (reciprocal) temperature of a single crystal. The inset shows the molar magnetic susceptibility vs. temperature, (χ_m in CGS-emu) [76L].

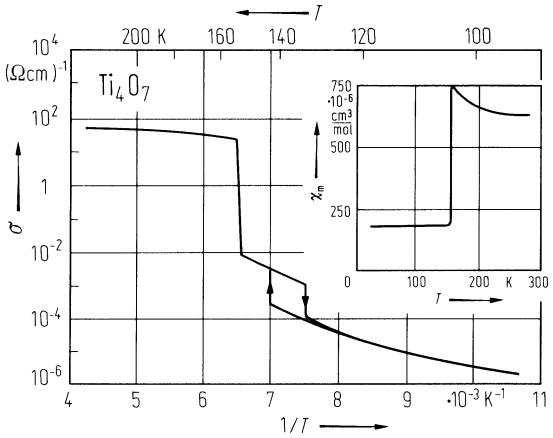

Fig. 3.

Ti_4O_7. Conductance ($1/R$) vs. temperature, showing fine structure in the hysteresis range. Sample was warmed through the 154 K transition between runs B and C which accounts for the ordinate displacement between the two hysteresis loops. In the as-grown state this sample had an exceptionally low ρ ($\approx 10^{-3}$ Ωcm) among the samples studied [83I].

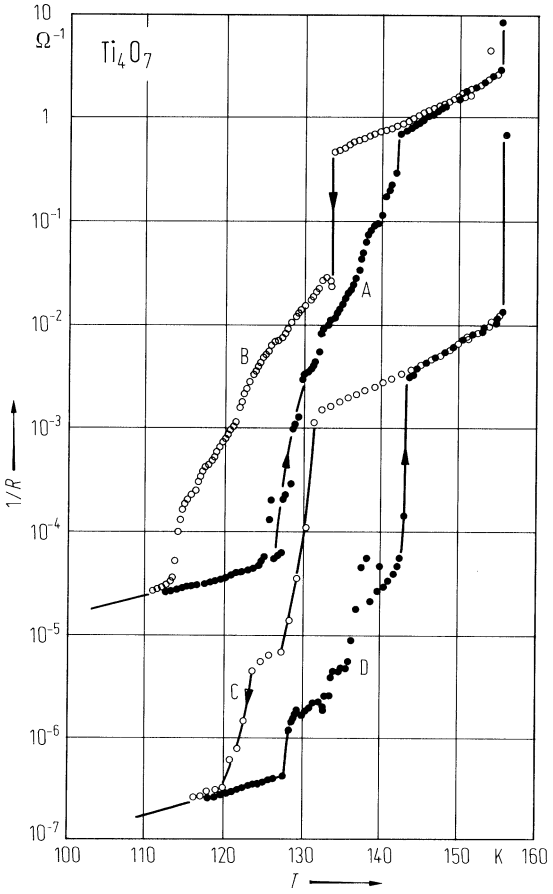

Fig. 4.

Ti_5O_9. Conductivity vs. reciprocal temperature for a single crystal [77M]. Inset shows transition range on an enlarged scale. Orientation not specified.

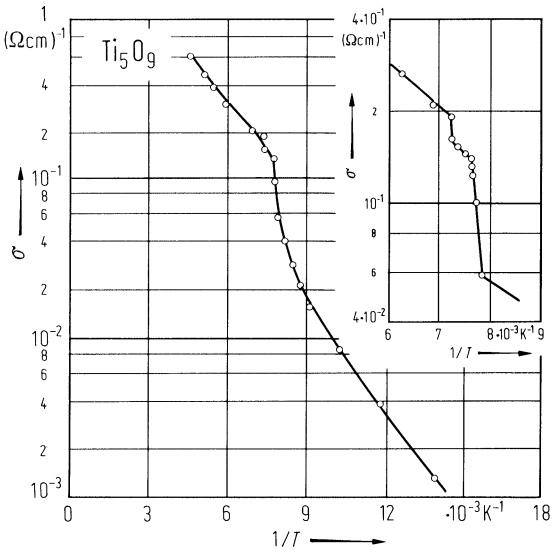

Fig. 5.

Ti_5O_9. Conductance vs. temperature for a single crystal. (a) shows detail of conductance in the transition region with clearly marked transition temperatures T_1, T_2, T_3; and (b) shows conductance over a wide temperature range; inset: low temperature range on an expanded scale [83I].

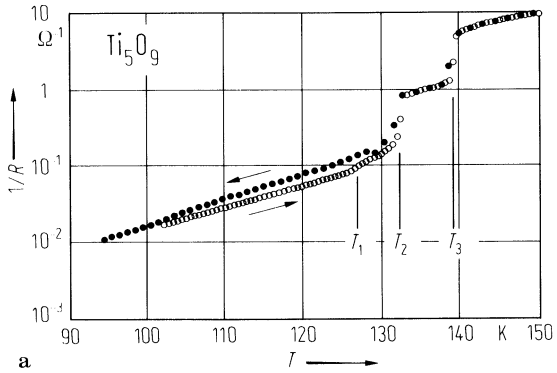

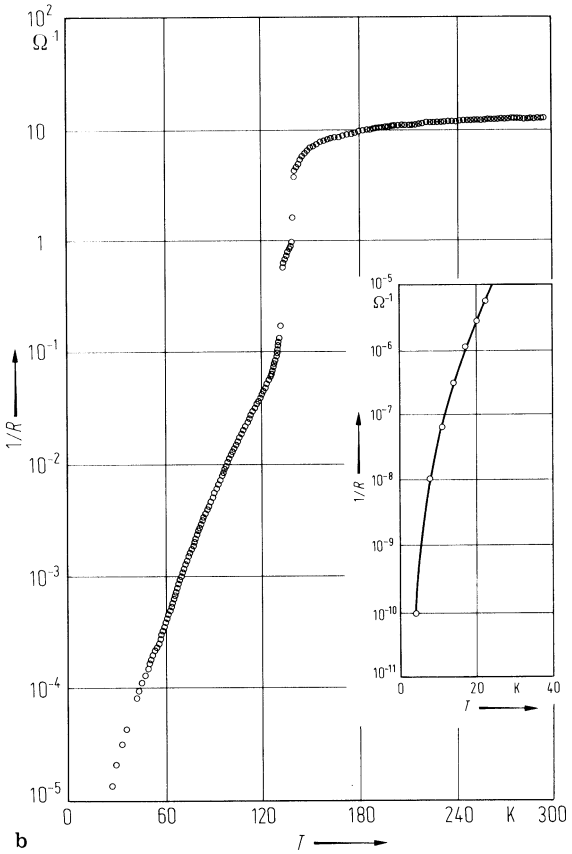

Fig. 6.

Ti_6O_{11}. Conductivity along *b*-axis vs. (reciprocal) temperature for a single crystal [69B].

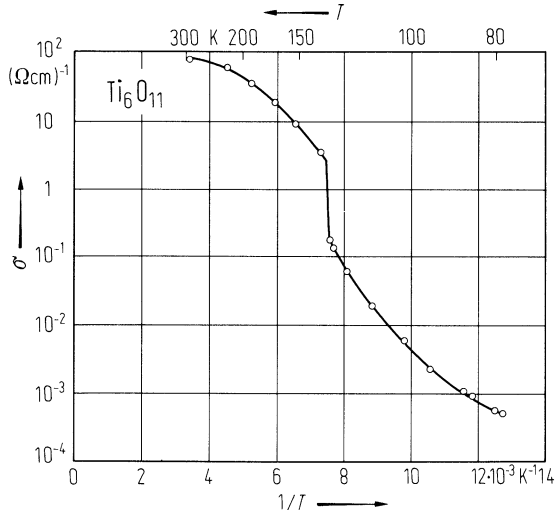

Fig. 7.

Ti_6O_{11}. Conductance vs. temperature. (a) shows detail of conductance in the transition region and (b) shows conductance over a wide temperature range; inset: low temperature range on an expanded scale [83I].

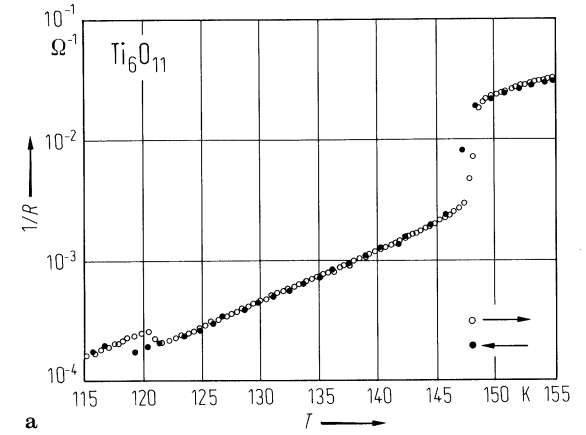

a

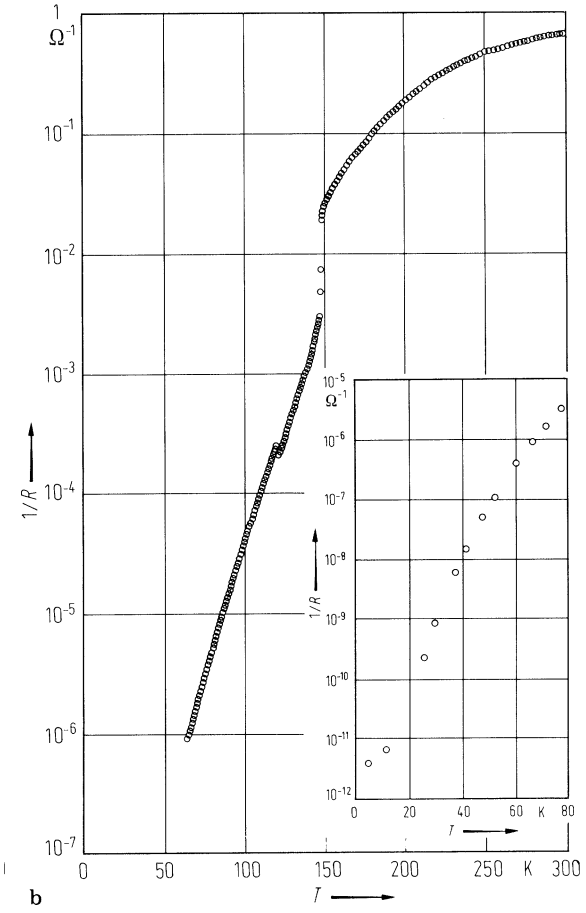

b

Fig. 8.

Ti_7O_{13}. Conductance vs. temperature. (a) shows detail of conductance in the transition region, (b) shows the conductance over a wide temperature range; inset: low temperature range on an expanded scale [83I].

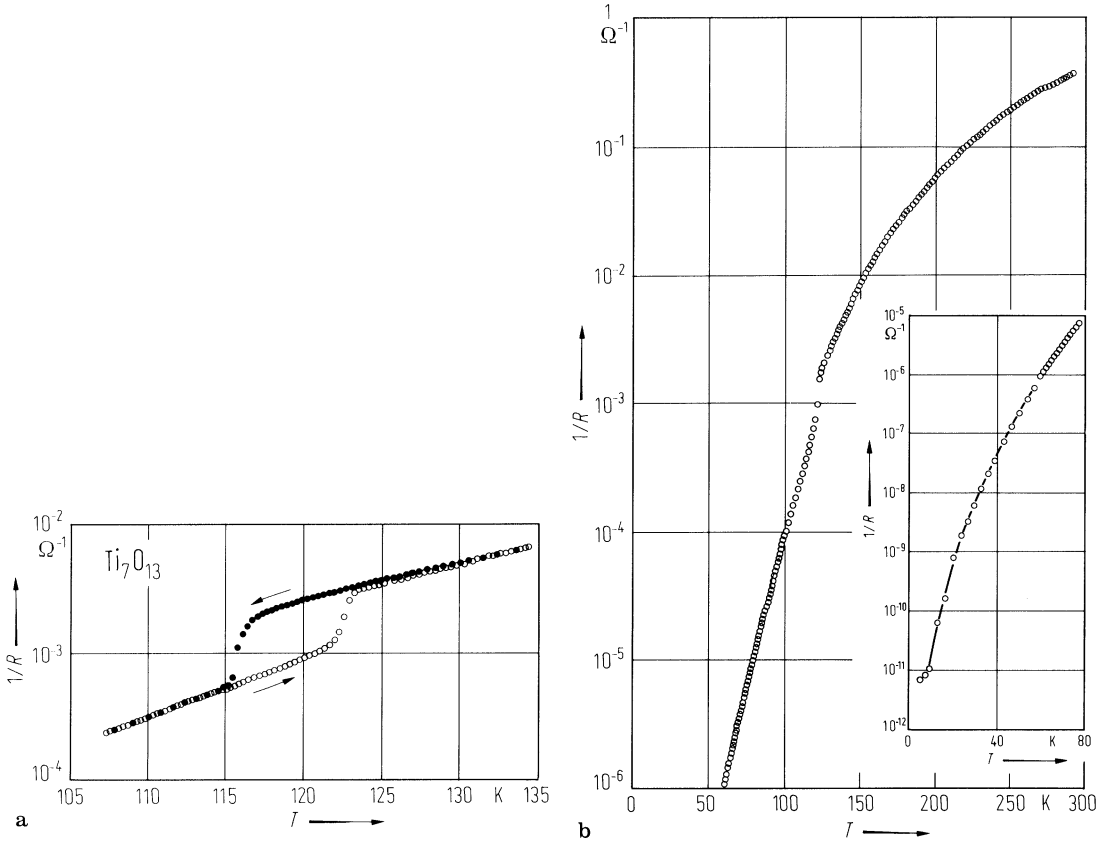

Fig. 9.

Ti_8O_{15}. Conductance vs. temperature. Evidence for a transition at 120 K comes from a discontinuity in d(1/*R*)/d*T* at that temperature. Insert shows low temperature range on an expanded scale [83I].

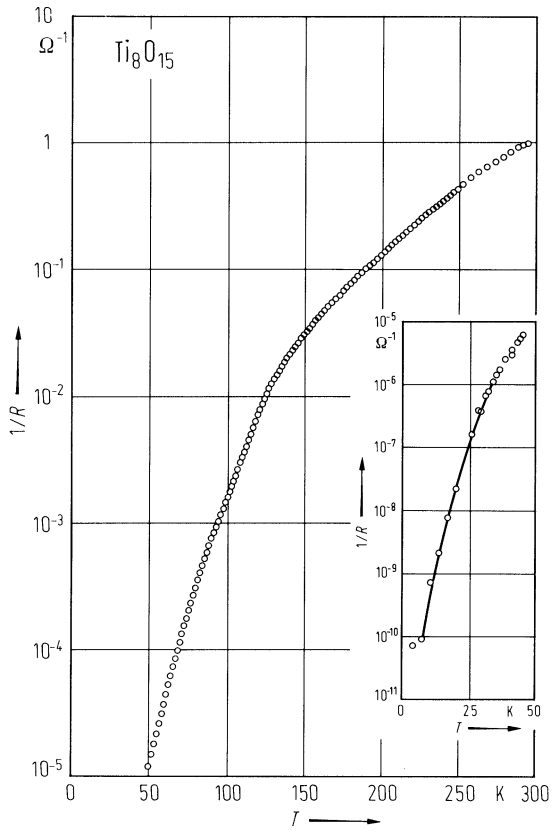

Fig. 10.

Ti_9O_{17}. Conductance vs. temperature. Insert shows low temperature range on an expanded scale [83I].